Experimental and numerical free vibration analysis of industry-driven woven fibre laminated glass/epoxy composite beams

Priyadarshi Das[1,2] and Shishir Kumar Sahu[1,3,*]

[1]Department of Civil Engineering, National Institute of Technology, Rourkela 769 008, India
[2]Department of Civil Engineering, Institute of Technical Education and Research, Siksha 'O' Anusandhan University, Bhubaneswar 751 030, India
[3]Centre for Nanomaterials, National Institute of Technology, Rourkela 769 008, India

The present study involves frequency-driven exploration of bi-directional, industry-driven, laminated composite glass/epoxy beams by experimental and finite element analysis. The experimental vibration responses were ensured through a vibration first Fourier transform (FFT) analyzer. The finite element predictions were made using MATLAB platform by developing a programmable computer code accounting for shear deformation. The results conclude that the free-vibration finite element predictions for glass/epoxy beams are sensitive to effects of different boundary conditions and span-to-thickness ratios. The present study will assist in our understanding of modal behaviour towards design and service of laminated beams in the frequency domain and can serve as experimental benchmark results.

Keywords: Finite element analysis, free vibration, laminated composite beam, modal behaviour, natural frequency.

THE laminated composites have high specific stiffness, tailorability, are cost-effective and lightweight. Thus they are used in aerospace, naval, civil and mechanical engineering applications[1–3]. With such widespread use, the laminated composite beams (LCBs) are repeatedly exposed to a wide range of dynamic and static loads accounting which degrade the functionality of structures. Towards structural stability and functionality of LCBs, strength, durability and loading aspects are important factors and hold a great extent of research significance. To this end, modal analysis of LCBs in the free vibration domain has pronounced technical importance with potential research attention. In this context, research studies are focused towards LCBs within the frequency domain.

The studies involving vibration of composite beams (CBs) contain a range of research approaches extending from basic analytical solutions to efficient and effective numerical methods. A compilation of such studies was presented by Kapania and Raciti[4]. A review of research regarding straight and curved composite beams in frequency threshold was conducted by Hajianmaleki and Qatu[5]. The traditional steel–concrete CBs have received significant research attention[6–10]. The analytical solutions reflected in different research studies for LCBs under free vibration are generally restricted to classical boundary conditions and simple geometries[11–13]. To overcome such limitations, finite element method (FEM), Ritz method, etc. have gained more attention now. Due to its acceptable accuracy with lower computational cost, FEM is used extensively as a powerful tool in structural analysis[14,15].

The classical lamination theory (CLT) does not account for any deformations due to shear and inaccurately predicts the natural frequencies[16]. Such limitations are countered through shear deformation approach using linear, quadratic and cubic elements to study the vibration of LCBs. The linear elements used in first-order shear-deformation theory (FSDT) are effective for predicting natural frequencies of structures without any damages or distortions. Thus, there is a good amount of research on the vibration of CBs for finite element (FE) predictions based on FSDT[17–19]. Goyal and Kapania[20] performed a dynamic exploration of unsymmetrical LCB adopting a shear deformable element with 21-DOF at each node. The commercial FE simulation software ANSYS was used to study the effect of mechanical and flexural properties and fibre orientation on the frequency of vibration of CBs[21]. Giunta *et al.*[22] explored the vibration behaviour of a cross-ply LCB using several higher-order and classical theories based on FEM. Kheladi *et al.*[23] explored the free-vibration behaviour of stiffened LCB. Several studies have been performed on the vibration of composite plates[24–26] and shells[27,28], given their broad applicability.

The vibration exploration of CBs tends to be a critical issue in laminated structures owing to the complex nature of lamination that involves orthotropy, ply-sequencing and stretching–bending–coupling. Relatively less studies dealing with free vibration of LCBs in modal domain through numerical and analytical analysis are available in the literature. In spite of the functional significance of laminated composites, the experimental research on free vibration of LCBs is limited and this realization was highlighted in the review study by Rafiee *et al.*[29]. The literature survey reveals the lack of a comprehensive understanding

*For correspondence. (e-mail: sksahu.nitrkl@gmail.com)

of the parametric effects on modal properties of laminated composites. Accentuating the experimental aspect, vibration studies on industry-driven woven fabric epoxy-based LCB are not addressed in the literature and thus, are the focus of the present study. Apart from experiments, a FEM-based computer program has been developed for linear beam model accounting for shear deformation in MATLAB platform for numerical modal testing of glass/epoxy LCB.

The enumerated contributions to the present study can be summed up as follows.

(i) Modal analysis for numerical computation of frequency responses is performed using FEM on MATLAB platform.
(ii) Within the modal domain, the experimental outcomes from first Fourier transform (FFT) analyzer show good agreement with the theoretical outcomes.
(iii) The research outcomes from the present study can be utilized by relating the modal frequencies to various parameters of LCBs for improving serviceability and structural functionality within this free vibration domain.

Mathematical formulation

The geometric signatures (length, width and thickness) along with the coordinate axes for a quintessential laminated beam are depicted in Figure 1, showing different layers of lamination. The LCB geometric signatures are L, b, and h, representing length, width and thickness respectively.

Finite element analysis

An eight-noded isoparametric beam element has been adopted for FE analysis and the formulation developed accounting for shear deformation.

To this end, based on FSDT displacement fields were assumed following Maiti and Sinha[17] as

$$u(x, y, z) = u_0(x, y) + z\theta_x, \tag{1}$$

$$v(x, y, z) = v_0(x, y) + z\theta_y, \tag{2}$$

$$w(x, y, z) = w_0(x, y), \tag{3}$$

where u, v and w are the components of displacement in the x, y, and z coordinate system respectively and u_0, v_0 and w_0 are the associated midplane displacement components respectively. θ_x and θ_y are in-plane rotations along the x–z and y–z plane respectively.

The strain energy for an intact beam is

$$U = \frac{1}{2}\int [\varepsilon]^T [B][\varepsilon]\mathrm{d}V, \tag{4}$$

where $[\varepsilon]$ is the strain tensor and the strain displacement is expressed as $[B]$ integrated over volume V.

Constitutive relations

The constitutive equations following FSDT for laminated composites are expressed as follows

$$\begin{Bmatrix} N_x \\ N_y \\ N_{xy} \\ M_x \\ M_y \\ M_{xy} \\ Q_{yz} \\ Q_{xz} \end{Bmatrix} = \begin{bmatrix} A_{11} & A_{12} & A_{16} & B_{11} & B_{12} & B_{16} & 0 & 0 \\ A_{21} & A_{22} & A_{26} & B_{21} & B_{22} & B_{26} & 0 & 0 \\ A_{16} & A_{26} & A_{66} & B_{16} & B_{26} & B_{66} & 0 & 0 \\ B_{11} & B_{12} & B_{16} & D_{11} & D_{12} & D_{16} & 0 & 0 \\ B_{21} & B_{22} & B_{26} & D_{21} & D_{22} & D_{26} & 0 & 0 \\ B_{16} & B_{26} & B_{66} & D_{16} & D_{26} & D_{66} & 0 & 0 \\ 0 & 0 & 0 & 0 & 0 & 0 & S_{44} & S_{45} \\ 0 & 0 & 0 & 0 & 0 & 0 & S_{45} & S_{55} \end{bmatrix} \begin{Bmatrix} \varepsilon_x^0 \\ \varepsilon_y^0 \\ \gamma_{xy} \\ \kappa_x \\ \kappa_y \\ \kappa_{xy} \\ \gamma_{yz} \\ \gamma_{xz} \end{Bmatrix}, \tag{5}$$

where the in-plane forces follow the notations N_x, N_y and N_{xy}, whereas the bending and twisting moments in the midplane are M_x, M_y and M_{xy}. κ_x, κ_y and κ_{xy} are associated with the curvatures of twisting and bending. The extensional, coupling and bending stiffnesses are A_{ij}, B_{ij} and D_{ij} respectively.

$$A_{ij} = \sum_{k=1}^{n} (\overline{Q_{ij}})_k (z_k - z_{k-1}),$$

$$B_{ij} = \frac{1}{2}\sum_{k=1}^{n} (\overline{Q_{ij}})_k (z_k^2 - z_{k-1}^2)z,$$

$$D_{ij} = \frac{1}{3}\sum_{k=1}^{n} (\overline{Q_{ij}})_k (z_k^3 - z_{k-1}^3),\ \ i, j = 1, 2, 6,$$

$$S_{ij} = k\sum_{k=1}^{n} (\overline{Q_{ij}})_k (z_k - z_{k-1}),\ \ i, j = 4, 5,$$

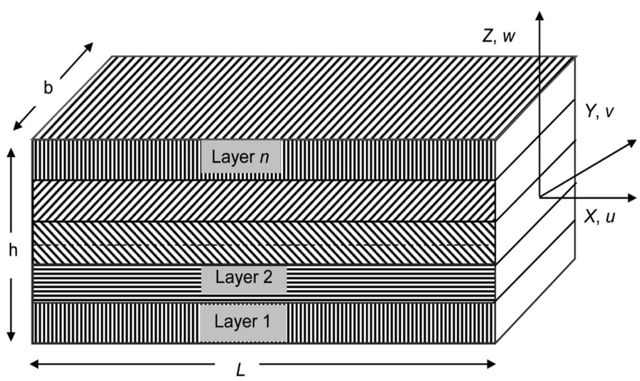

Figure 1. Geometry of laminated composite beam (LCB).

where $\overline{Q_{ij}}$ is the reduced off-axis stiffnesses (for $i, j = 1, 2, 6$), S_{ij} the transverse shear stiffnesses and k is the shear correction factor (we have adopted a value of 5/6 in line with refs 12, 17).

The y-axis force and moment components are neglected assuming no axial force and thus, the strains are also zero. So, the expression for the constitutive equation is

$$\begin{Bmatrix} M_x \\ Q_{xz} \end{Bmatrix} = \begin{bmatrix} D_{11} & 0 \\ 0 & S_{55} \end{bmatrix} \begin{Bmatrix} \kappa_x \\ \gamma_{xz} \end{Bmatrix}. \quad (6)$$

Solution to element matrices

Towards governing the eigen frequencies, the mass matrix (M_e) and beam element stiffness matrix (K_e) are expressed for free vibration through FE analysis as

$$M_e = \int_{-1}^{+1}\int_{-1}^{+1} [N]^T [P][N] \, |J| \, \mathrm{d}\xi \mathrm{d}\eta, \quad (7)$$

$$K_e = \int_{-1}^{+1}\int_{-1}^{+1} [B]^T [D][B] \, |J| \, \mathrm{d}\xi \mathrm{d}\eta, \quad (8)$$

where $[N]$ represents shape function and $|J|$ is the Jacobian determinant. The stress–strain matrix $[D]$ is expressed as

$$[D] = \begin{bmatrix} D_{11} & 0 \\ 0 & S_{55} \end{bmatrix}. \quad (9)$$

The components of $[N]$ for an eight-noded isoparametric beam element are

$$N_i = \frac{1}{4}(\xi^2 + \xi\xi_i)(\eta^2 + \eta\eta_i), \; i = 1, 2, 3, 4,$$

$$N_i = \frac{1}{2}(1 - \xi^2)(\eta^2 + \eta\eta_i), \; i = 5, 7,$$

$$N_i = \frac{1}{2}(\xi^2 + \xi\xi_i)(1 - \eta^2), \; i = 6, 8,$$

$[P]$ is the inertia matrix and for FSDT it is expressed as

$$[P] = \begin{bmatrix} I & 0 & 0 & P_1 & 0 \\ 0 & I & 0 & 0 & P_1 \\ 0 & 0 & I & 0 & 0 \\ P_1 & 0 & 0 & Q & 0 \\ 0 & P_1 & 0 & 0 & Q \end{bmatrix},$$

where $(I, P_1, Q) = \int_{-h/2}^{h/2} (1, z, z^2)\rho(z) \, \mathrm{d}z.$

Eigen solution

The eigen frequencies for free vibration can be governed using the following expression

$$|[K] - \omega^2[M]| = 0, \quad (10)$$

where $[K]$ and $[M]$ are the stiffness and mass matrix respectively, while ω is the natural frequency. Based on eq. (10), the MATLAB code has been developed. Figure 2 shows a flow chart for the MATLAB program.

Experimental analysis

The experimental modal analysis was performed on glass/epoxy CB samples made up in a proportion of 50 : 50 by weight of scissored glass fabrics (Owens Corning-360 g/m^2, WR 360/100) on a epoxy resin matrix. A blend of 90% epoxy (Lapox L-12, Atul Ltd, India) with 10% hardener (K-6, Atul Ltd, India) was used for epoxy resin matrix preparation. The fabrication was done on a flat, smooth, wooden plate employing the hand lay-up technique[24,30]

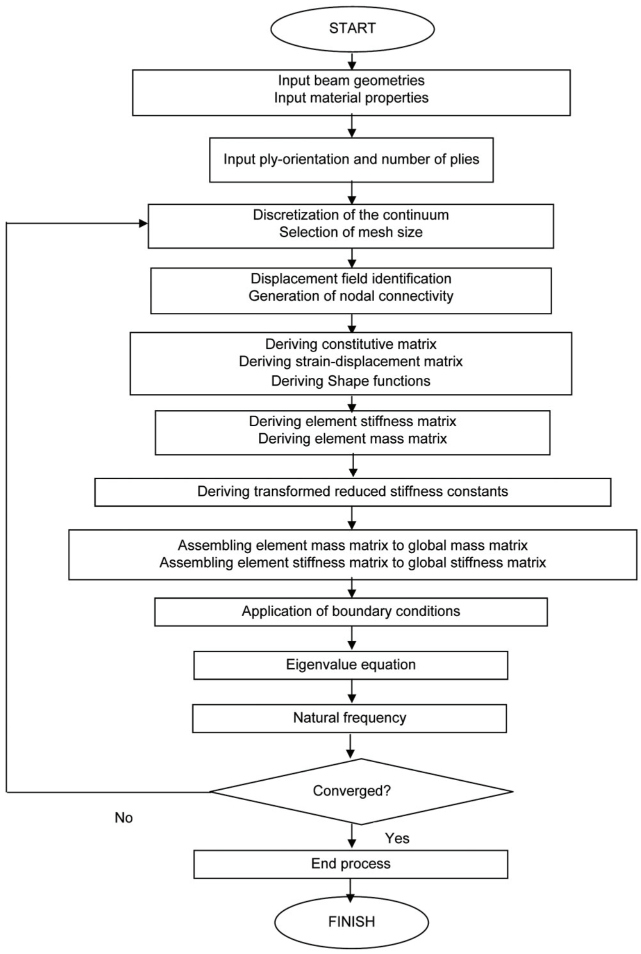

Figure 2. Flow chart of MATLAB program for free vibration of LCB.

(Figure 3 *a*). Prior to fibre lamination, a thin plastic releasing sheet was placed on the mould sprayed with the releasing agent (silicone spray). The laminated plate was then placed under heavy flat iron loads for curing at room temperature. On curing, the LCB specimens were generated from the fabricated composite plate using a diamond cutter. The geometrical signatures of the glass/epoxy LCB measured 2500 mm longitudinally (L), 25 mm in width (b) and the thickness (h) was measured using a Vernier caliper as 3.2 mm. Figure 3 *b* shows the beam samples.

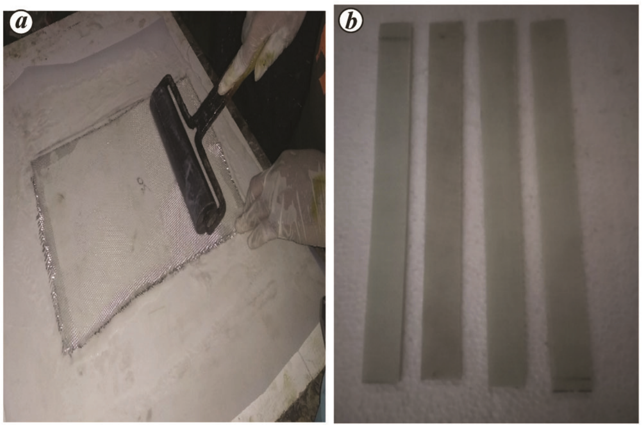

Figure 3. LCB fabrication: (***a***) hand lay-up and (***b***) produced beam samples.

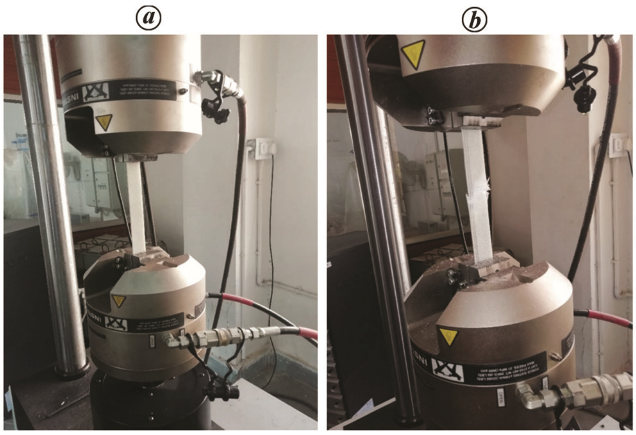

Figure 4. Tensile testing of glass/epoxy LCB in INSTRON 8862: (***a***) specimen before failure and (***b***) specimen after failure.

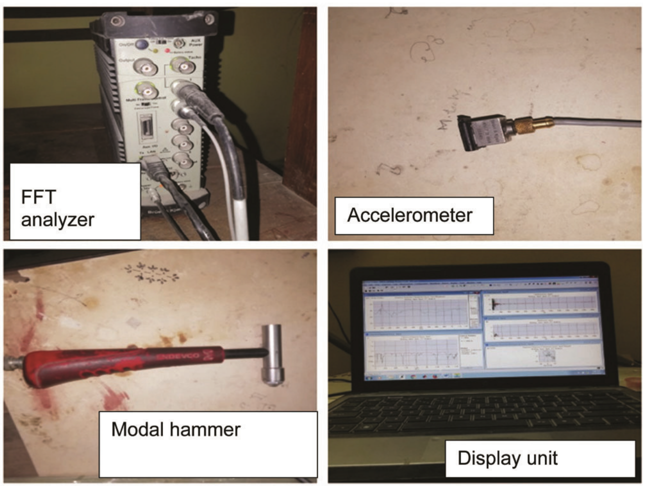

Figure 5. Complete experimental set-up.

Tensile test for evaluation of material constants

The Young's moduli E_{11}, E_{22} ($E_{11} = E_{22}$ in this study), and Poisson's ratio ν_{12} of the laminated composite glass/epoxy beams were determined experimentally from the tensile tests. The LCB samples were paced in the Universal Testing Machine (UTM) INSTRON 8862 set-up (Figure 4 *a*), and following the procedures elaborated in ref. 31, the unidirectional test was performed for material constant evaluation (Figure 4 *b*).

Here, E_{45} denotes the elastic property of the laminated beam cast at 45° to the longitudinal direction.

The shear modulus G_{12} was computed according to ref. 32.

$$G_{12} = \frac{1}{\frac{4}{E_{45}} - \frac{1}{E_1} - \frac{1}{E_2} + \frac{2\nu_{12}}{E_1}}. \tag{11}$$

Table 1 summarizes the material elasticities from the tensile test.

Modal analysis

The frequency measurements were done for glass/epoxy LCB subjected to free vibration test for different boundary conditions. The support conditions were assigned and confirmed by means of an iron frame exclusively fabricated for this purpose. A set of vibration tests was performed using the FFT analyzer for composite laminated

Table 1. The woven fibre glass/epoxy laminated composite beam (LCB) material properties

Material properties		Test results
Modulus of elasticity	E_{11}	15.71 GPa
	E_{22}	15.71 GPa
	E_{45}	2.94 GPa
Poisson's ratio	ν_{12}	0.28
	ν_{13}	0.28
	ν_{23}	0.28
Modulus of rigidity	G_{12}	2.964 GPa
	G_{13}	2.964 GPa
	G_{23}	2.964 GPa
Mass density	ρ_m	1644.65 kg/m^3

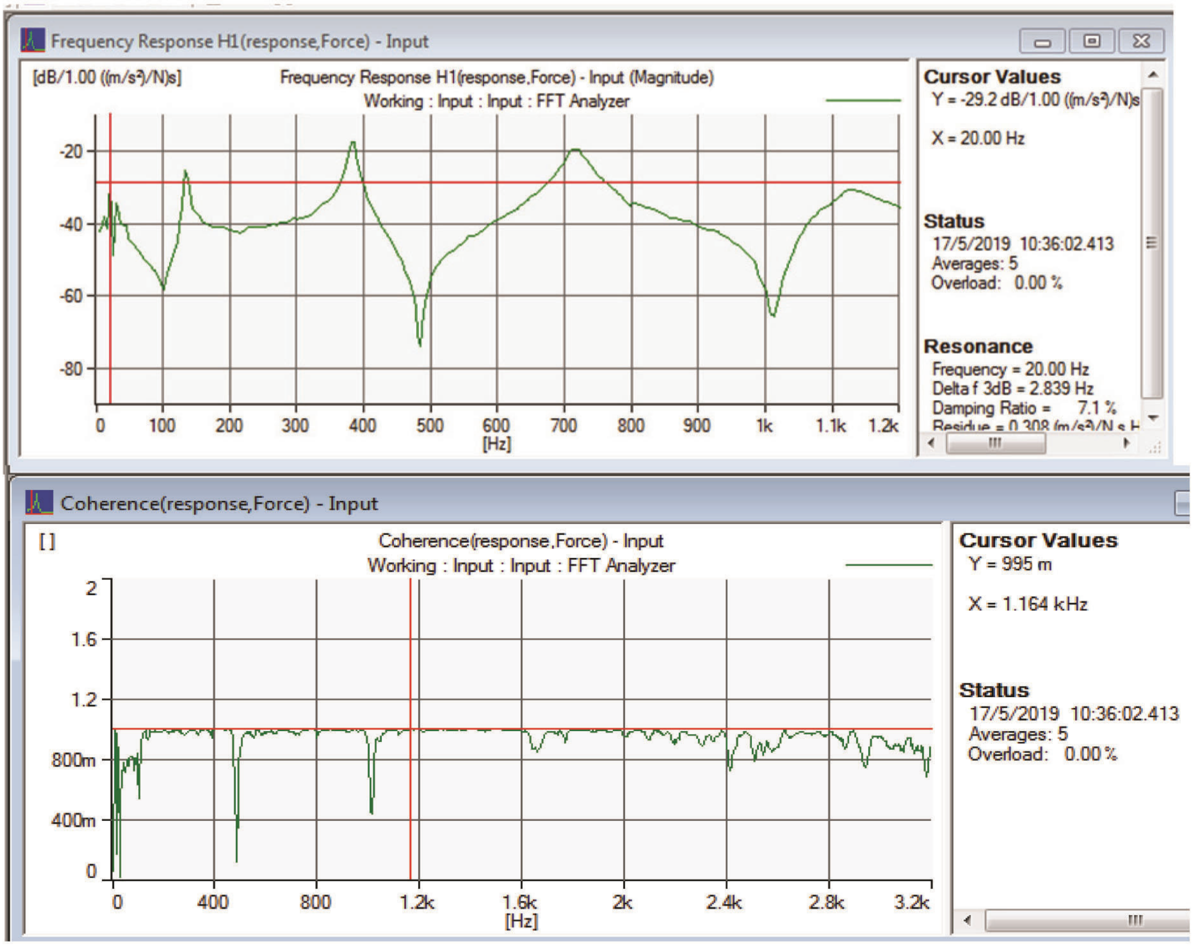

Figure 6. Frequency response functions and coherence graph for clamped-free beam with 0° fibre orientation.

Table 2. Convergence of clamped-free (CF) composite beam frequencies under free vibration

	Natural frequency (Hz) for different fibre angle (θ, deg)			
Mesh division	$\theta = 0°$	$\theta = 15°$	$\theta = 30°$	$\theta = 45°$
4 × 1	273.9	246.69	163.2	96.31
8 × 1	273.88	246.43	162.4	95.81
12 × 1	273.86	246.36	162.02	95.56
16 × 1	273.85	246.35	161.92	95.11
Ref. 18	278.5	209.5	140.0	90.8

$E_1 = 144.8$ GPa, $E_2 = E_3 = 9.65$ GPa, $G_{12} = G_{13} = 4.14$ GPa, $G_{23} = 3.45$ GPa, $\nu = 0.3$, $\rho = 1389.23$ kg/m^3, $L = 0.381$ m, $b = 0.0254$ m, $h = 0.0254$ m.

Table 3. Comparison of non-dimensional fundamental frequencies

	CC		CF		SS	
Lamination	Present FEM	Ref. 17	Present FEM	Ref. 17	Present FEM	Ref. 17
0/90/0/90	55.4222	55.9998	8.8418	8.8538	26.3157	26.3783
0/30/-30/0	76.8977	77.9663	12.4001	12.4044	34.6808	34.7859
0/45/-45/0	75.9531	77.0865	12.2661	12.2714	34.2911	34.4025
0/60/-60/0	75.4649	76.7132	12.2167	12.2266	34.1501	34.2714

CC, Clamped-clamped; CF, Clamped-free; SS, Simply-supported. $\lambda = \omega(L^2/h)(\sqrt{(\rho * 12)/E_2})$ for LCB ($L/h = 60$). $E_1 = 129.207$ GPa; $E_2 = E_3 = 9.42512$ GPa; $G_{12} = 5.15658$ GPa; $G_{13} = 4.3053$ GPa; $G_{23} = 2.5414$ GPa; $\nu_{12} = \nu_{13} = 0.3$; $\nu_{23} = 0.218837$; $\rho = 1550.0666$ kg/m^3; $L = 0.1905$ m and $b = 0.0127$ m.

beams. Figure 5 presents the required components of the experimental modal testing. The over-mount accelerometer (B&K 4507 B) was attached to the surface of the LCB and excited in five-frames in its vicinity through an impact modal hammer (B&K 2302-5 B). The excited signals received by the sensor were processed using the FFT analyzer (B&K 3560 B) and the recorded frequency response was exhibited on the system using PULSE lap-shop compatible universal software. The frequency spectrum was displayed in the domain for five frequency response functions (FRFs). The precession of the measurement was reflected in the coherence curve that exhibited a value closer to unity. Figure 6 presents the FRFs with coherence for the glass/epoxy LCB with cantilever or clamped-free (CF) support condition and 0° fibre orientation.

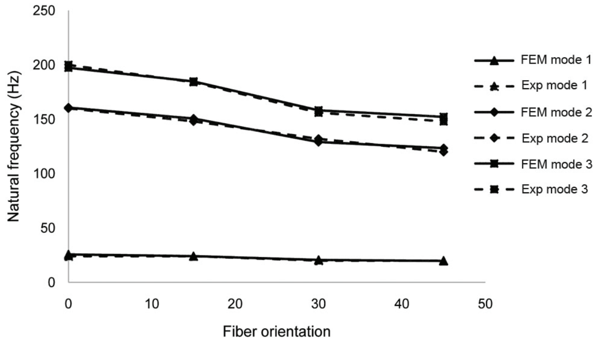

Figure 7. Variation in vibration frequencies of cantilever LCB for different fibre angles.

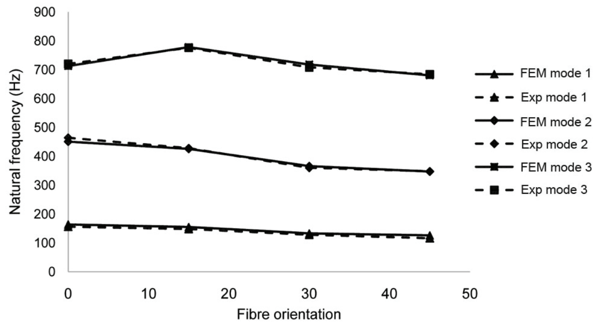

Figure 8. Variation in vibration frequencies of fixed LCB for different fibre angles.

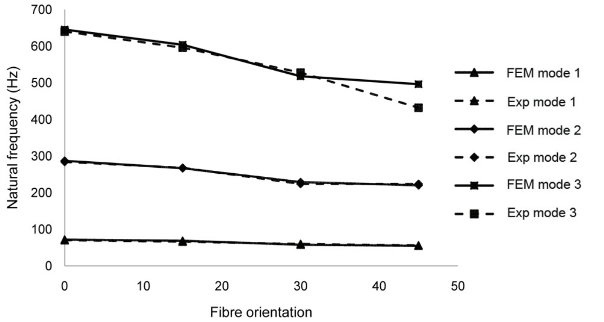

Figure 9. Variation in vibration frequencies of simply-supported LCB for different fibre angles.

Results and discussion

The FE predictions for eigenvalue frequencies were computed through MATLAB simulation and experimental work through FFT analyzer. The recorded results for frequencies of free vibration are discussed through following ways as: (i) convergence study, (ii) comparison study and (3) new experimental and FE analysis results.

Convergence study

The convergence study was performed to select a suitable mesh size that governs the optimal result (Table 2). In this context, exact beam parameters were considered as used by Talekar and Kotambkar[18]. From Table 2, we can observe a convergence of results for a mesh division of 16×1, and thus, this mesh size was utilized for further vibration analysis.

Comparison with previous studies

The FE predictions were compared with those of Maiti and Sinha[17] (Table 3). The material properties and support conditions were considered in line with those of Maiti and Sinha[17]. Table 3 indicates the similarity between the present FE predictions and the published results. This affirms the proficiency of the FE formulation used in the present study.

Experimental and numerical modal results

The modal frequencies under free vibration for glass/epoxy LCB were recorded through FE analysis as well as from experiments. The beam geometries were chosen as mentioned earlier and the beam elastic constants were confirmed from Table 1.

In the present study, the following parameters have been considered in the threshold of free vibration.

- The effect of different boundary conditions.
- The effect of span-to-depth ratio.

Free vibration of glass/epoxy LCB with respect to different boundary conditions: Figures 7–9 show the shift in frequency response of glass/epoxy LCB with different boundary conditions. For assessment of the effect of different boundary conditions (BC) on the natural frequencies of LCB, CF, CC (clamped-clamped) and SS (simply supported) cases were considered. The experimental and numerical analyses were carried out for [0/0/0/0]s, [15/-15/-15/15]s, [30/-30/-30/30]s, and [45/-45/-45/45]s laminated beams (Figures 7–9). Analysing the CF support condition, Figure 7 shows that [45/-45/-45/45]s fibre orientation represents a 23% decrease in fundamental frequency and a 30% decrease in third natural frequency to [0/0/0/0]s fibre orientation. Similar observations are made from Figures 8 and 9 for CC and SS boundary conditions respectively. It can be noticed that as the ply-orientation increases from 0°, the frequency decreases for all the considered support conditions. This is also supported by similar observations by Jafari-Talookolaei *et al.*[12]. Also, it is evident from Figure 7 that the first three natural frequencies for CF boundary conditions showing lesser magnitude than other three boundary conditions. In contrast, the frequency of vibration shows maximum magnitude for CC. The restrained edges could be the reason for increased natural frequencies of free vibration.

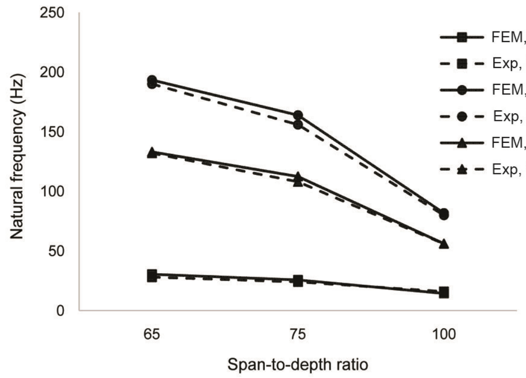

Figure 10. Variation in first-mode frequency with respect to *L*/*h* ratio for LCB with 0° fibre orientation.

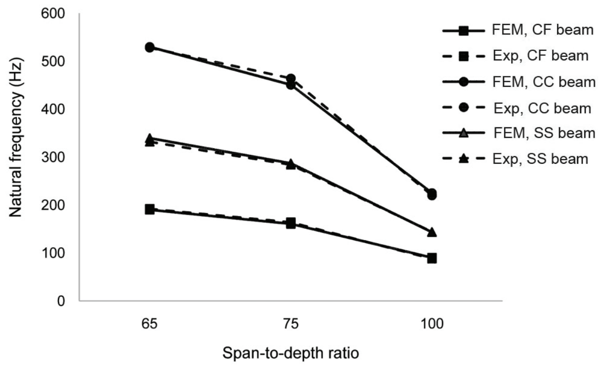

Figure 11. Variation in second-mode frequency with respect to *L*/*h* ratio for LCB with 0° fibre orientation.

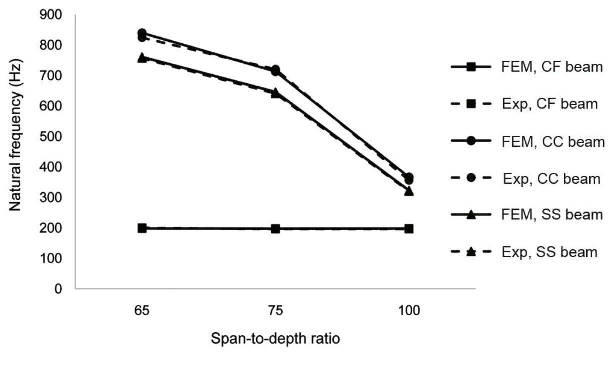

Figure 12. Variation in third-mode frequency with respect to *L*/*h* ratio for LCB with 0° fibre orientation.

Free vibration of glass/epoxy LCB with respect to different span-to-depth ratios: Figures 10–12 demonstrates alterations in natural frequency of glass/epoxy LCB due to varying *L*/*h* ratio. Three different LCBs were fabricated in this context, confirming *L*/*h* ratios 100, 75, and 50 with 0° fibre orientation. The material properties were secured to the values given in Table 1, i.e. length (*L*) = 250 mm and width (*b*) = 25 mm. The vibration frequencies using experimental work and numerical computation have been graphically represented in Figures 10, 11 and 12 for CF, CC and SS support conditions respectively. The experimental and numerical results show close resemblance, and thus, good agreement is established. The graphs demonstrate that for a small *L*/*h* value the fundamental frequency increases. Figure 10 shows that the fundamental frequency spectrum varies from 79% to 100% for *L*/*h* ratio 75, compared to *L*/*h* ratio 100. Further, it increases by 15–18% for CB with *L*/*h* = 65. From Figures 11 and 12, it is observed that the higher mode frequencies of composite beam with *L*/*h* = 65 exhibit greater magnitude than the higher mode frequencies of beam with *L*/*h* = 75 and *L*/*h* = 100. As expected, the higher modes of different *L*/*h* ratios yield similar results for FSDT and CLT[11,12]. This outcome shows that the aspect ratio significantly impacts the natural frequency, and as reported by Jafari-Talookolaei *et al.*[12].

Conclusion

In the present analysis, both experimental and numerical approaches are presented to address the free vibration analysis of industry-driven, woven fibre glass/epoxy LCB. The FE predictions in MATLAB environment considering the effects of support conditions and span-to-depth ratios have been validated experimentally using the FFT analyzer. Following conclusions can be made from the present study:

- The experimental test results are in acceptable agreement with the FE predictions made using the MATLAB platform.
- The maximum value of natural vibration frequency was recorded for the CC beam, whereas minimum was observed for LCB with CF support conditions.
- The nature of the supports at the edges influences the free vibration frequencies. Due to the rigid condition at both the ends, the fixed beams show significantly higher frequencies than other types of beams.
- As the ply-orientation is increased gradually, a significant variation in frequencies of vibration for higher modes are detected.
- For different sets of lamination sequences, LCB with 0° orientation displays greater vibration responses for all adopted boundary conditions.
- The LCB frequencies are significantly affected as the aspect ratio increases.

Thus the vibration responses are significantly influenced by end supports, geometry, fibre orientation and sequencing in lamination. In particular, the experimental modal results can be regarded as a benchmark for researchers and designers in the field of composite laminates. The test results may prove helpful in non-destructive health assessment studies concerning composites in free vibration domain.

Conflicts of interest: The authors declare no conflict of interest.

1. Sinaei, H., Jumaat, M. Z. and Shariati, M., Numerical investigation on exterior reinforced concrete beam–column joint strengthened by composite fiber reinforced polymer (CFRP). *Int. J. Phys. Sci*., 2011, **6**(28), 6572–6579.
2. Shariati, M., Sulong, N. R., Shariati, A. and Khanouki, M. A., Behavior of V-shaped angle shear connectors: experimental and parametric study. *Mater. Struct*., 2016, **49**(9), 3909–3926.
3. Xie, Q., Sinaei, H., Shariati, M., Khorami, M., Mohamad, E. T. and Bui, D. T., An experimental study on the effect of CFRP on behavior of reinforce concrete beam column connections. *Steel Compos. Struct.*, 2019, **30**(5), 433–441.
4. Kapania, R. K. and Raciti, S., Recent advances in analysis of laminated beams and plates. Part II: vibrations and wave propagation. *AIAA J.,* 1989, **27**(7), 935–946.
5. Hajianmaleki, M. and Qatu, M. S., Vibrations of straight and curved composite beams: a review. *Compos. Struct.*, 2013, **100**, 218–232.
6. Shariati, A., Sulong, N. H., Suhatril, M. and Shariati, M., Investigation of channel shear connectors for composite concrete and steel T-beam. *Int. J. Phys. Sci*., 2012, **7**(11), 1828–1831.
7. Shariati, M., Sulong, N. R., Shariati, A. and Kueh, A. B. H., Comparative performance of channel and angle shear connectors in high strength concrete composites: an experimental study. *Constr. Build. Mater*., 2016, **120**, 382–392.
8. Safa, M., Shariati, M., Ibrahim, Z., Toghroli, A., Baharom, S. B., Nor, N. M. and Petkovic, D., Potential of adaptive neuro fuzzy inference system for evaluating the factors affecting steel–concrete composite beam's shear strength. *Steel Compos. Struct.*, 2016, **21**(3), 679–688.
9. Frederick, F. F., Sharma, U. K. and Gupta, V. K., Influence of end anchorage on shear strengthening of reinforced concrete beams using CFRP composites. *Curr. Sci.*, 2017, **112**(5), 973–981.
10. Shariati, M., Grayeli, M., Shariati, A. and Naghipour, M., Performance of composite frame consisting of steel beams and concrete filled tubes under fire loading. *Steel Compos. Struct.*, 2020, **36**(5), 587–602.
11. Krishnaswamy, S., Chandrashekhara, K. and Wu, W. Z. B., Analytical solutions to vibration of generally layered composite beams. *J. Sound Vib.*, 1992, **159**(l), 85–99.
12. Jafari-Talookolaei, R. A., Abedi, M., Kargarnovin, M. H. and Ahmadian, M. T., An analytical approach for the free vibration analysis of generally laminated composite beams with shear effect and rotary inertia. *Int. J. Mech. Sci*., 2012, **65**(1), 97–104.
13. Fazeli, S., Stokes-Griffin, C., Gilbert, J. and Compston, P., An analytical solution for the vibrational response of stepped smart cross-ply laminated composite beams with experimental validation. *Compos. Struct*., 2021, **266**, 113823.
14. Truong-Thi, T., Vo-Duy, T., Ho-Huu, V. and Nguyen-Thoi, T., Static and free vibration analyses of functionally graded carbon nanotube reinforced composite plates using CS-DSG3. *Int. J. Comput. Methods*, 2020, **17**(3), 1850133.
15. Koutoati, K., Mohri, F. and Carrera, E., A finite element approach for the static and vibration analyses of functionally graded material viscoelastic sandwich beams with nonlinear material behavior. *Compos. Struct*., 2021, **274**, 114315.
16. Abarcar, R. B. and Cunniff, P. F., The vibration of cantilever beams of fiber reinforced material. *J. Compos. Mater.*, 1972, **6**(4), 504–517.
17. Maiti, D. K. and Sinha, P. K., Bending and free vibration analysis of shear deformable laminated composite beams by finite element method. *Compos. Struct.*, 1994, **29**(4), 421–431.
18. Talekar, N. and Kotambkar, M., Free vibration analysis of generally layered composite beam with various lay-up and boundary conditions. *Mater. Today, Proc.*, 2020, **21**, 1283–1292.
19. Eyvazian, A., Musharavati, F., Tarlochan, F., Pasharavesh, A., Rajak, D. K., Husain, M. B. and Tran, T. N., Free vibration of FG-GPLRC conical panel on elastic foundation. *Struct. Eng. Mech*., 2020, **75**(1), 1–18.
20. Goyal, V. K. and Kapania, R. K., A shear-deformable beam element for the analysis of laminated composites. *Finite Elem. Anal. Des.*, 2007, **43**(6–7), 463–477.
21. Topcu, M. *et al*., Stacking sequence effects on natural frequency of laminated composite beams. *Adv. Compos. Lett*., 2008, **17**, 7–13.
22. Giunta, G., Biscani, F., Belouettar, S., Ferreira, A. J. M. and Carrera, E., Free vibration analysis of composite beams via refined theories. *Compos. B, Eng.*, 2013, **44**(1), 540–552.
23. Kheladi, Z., Hamza-Cherif, S. M. and Ghernaout, M. E. A., Free vibration analysis of variable stiffness laminated composite beams. *Mech. Adv. Mater. Struct*., 2020, **28**(18), 1–28.
24. Prasad, E. V. and Sahu, S. K., Vibration analysis of woven fiber metal laminated plates – experimental and numerical studies. *Int. J. Struct. Stab. Dyn*., 2018, **18**(11), 1850144.
25. Nguyen-Minh, N., Tran-Van, N., Bui-Xuan, T. and Nguyen-Thoi, T., Free vibration analysis of corrugated panels using homogenization methods and a cell-based smoothed Mindlin plate element (CS-MIN3). *Thin-Walled Struct.,* 2018, **124**, 184–201.
26. Patel, A., Das, R. and Sahu, S. K., Experimental and numerical study on free vibration of multiwall carbon nanotube reinforced composite plates. *Int. J. Struct. Stab. Dyn.*, 2020, **20**(12), 2050129.
27. Nguyen-Thoi, T., Bui-Xuan, T., Liu, G. R. and Vo-Duy, T., Static and free vibration analysis of stiffened flat shells by a cell-based smoothed discrete shear gap method (CS-FEM-DSG3) using three-node triangular elements. *Int. J. Comput. Methods*, 2018, **15**(06), 1850056.
28. Biswal, M., Sahu, S. K. and Asha, A. V., Experimental and numerical studies on free vibration of laminated composite shallow shells in hygrothermal environment. *Compos. Struct.*, 2015, **127**, 165–174.
29. Rafiee, M., Nitzsche, F. and Labrosse, M., Dynamics, vibration and control of rotating composite beams and blades: a critical review. *Thin-Walled Struct.*, 2017, **119**, 795–819.
30. Das, P. and Sahu, S. K., Free vibration analysis of industry-driven woven fiber laminated carbon/epoxy composite beams by experimental and numerical approach. *Polym. Polym. Compos.*, 2021, **29**, 1371–1385.
31. ASTM (2008) D 3039/D 3039M, Standard test method for tensile properties of polymer matrix composite materials. ASTM International, West Conshohocken, PA, USA, 2008.
32. Jones, R. M., *Mechanics of Composite Materials*, CRC Press, Philadelphia, USA, 1998.

Received 8 January 2021; revised accepted 5 February 2022

doi: 10.18520/cs/v122/i9/1058-1065